Yanbo Yang
Clean Energy Automotive Engineering Center,
School of Automotive Studies,
Tongji University,
No. 4800, Caoan Road,
Shanghai 201804, China
e-mail: yanboyang@tongji.edu.cn

Tiancai Ma[1]
Clean Energy Automotive Engineering Center,
School of Automotive Studies,
Tongji University,
No. 4800, Caoan Road,
Shanghai 201804, China
e-mail: matiancai@tongji.edu.cn

Fenglai Pei
Shanghai Motor Vehicle Inspection Certification
and Tech Innovation Center Co., Ltd.,
No. 68, South Yutian Road,
Shanghai 201804, China
e-mail: fenglaip@smvic.com.cn

Weikang Lin
Clean Energy Automotive Engineering Center,
School of Automotive Studies,
Tongji University,
No. 4800, Caoan Road,
Shanghai 201804, China
e-mail: weikang.lin@tongji.edu.cn

Kai Wang
Clean Energy Automotive Engineering Center,
School of Automotive Studies,
Tongji University,
No. 4800, Caoan Road,
Shanghai 201804, China
e-mail: wangkai3933@163.com

Boyu Du
Clean Energy Automotive Engineering Center,
School of Automotive Studies,
Tongji University,
No. 4800, Caoan Road,
Shanghai 201804, China
e-mail: duboyu@tongji.edu.cn

Study on the Degradation Mechanism of the Proton Exchange Membrane Fuel Cell Based on a Constant Voltage Cold Start Mode

The constant voltage cold start of the proton exchange membrane fuel cell (PEMFC) is usually operated at a low start-voltage in order to ensure high heat generation, which can shorten the process of the PEMFC cold start. However, the effect of constant voltage cold start on the durability of PEMFC is still unclear. Thus, in this work, the PEMFC is tested repeatedly at a low start-voltage to simulate its actual operating state in the vehicle. Then, the effect of the PEMFC durability under constant voltage cold start is investigated by polarization curve, cyclic voltammetry, electrochemical impedance spectroscopy, transmission electron microscope, and ion chromatography. After the repeatedly cold start, the output performance of the PEMFC decreases significantly. According to the characterization results, the degradation mechanism of the PEMFC at the constant voltage cold start is demonstrated to be that the PEMFC start-up repeatedly at low start-voltage leads to the decomposition of membrane polymer structure and promotes the crossover of H_2. Meanwhile, the PEMFC start-up repeatedly at low start-voltage also leads to the agglomeration of catalysts, which reduces the active area of catalysts and ultimately results in the degradation of fuel cell performance. Above all, this study proves that the durability of PEMFC can be shortened by the constant voltage cold start at 0.1 V, which provides a reference for the development of the PEMFC cold start control strategy. [DOI: 10.1115/1.4052534]

Keywords: proton exchange membrane fuel cell, cold start, constant voltage mode, degradation

Introduction

Proton exchange membrane fuel cell (PEMFC), as an efficient hydrogen energy utilization device, has attracted much attention for its high efficiency, environment friendly, and so on [1–3]. However, there are still some problems in the cold start of the PEMFC greatly restricting its commercialization [4]. Detailedly, in the subfreezing temperature environment, the water generated by the electrochemical reaction is easy to freeze on the surface of the catalytic layer (CL) and the gas diffusion layer (GDL) of the membrane electrode assembly (MEA) in the fuel cell [5]. Meanwhile, the formed ice can obstruct the gas transmission and even cause the failure of the electrochemical reaction, thus leading to the cold start failure [6,7]. Therefore, promoting the performance of the cold start and durability of PEMFC is significant for prolonging its lifetime and breaking the limits of its commercial application.

In the past decades, several studies have been carried out to illuminate the freezing mechanism and cold start process of PEMFC, which offer theoretical evidence to realize the cold start of PEMFC at subzero temperature environments [8–11]. Jiao et al. [9], for instance, found that CL and GDL of the cathode were much likely to freeze during the cold start of the PEMFC, which led to the failure of the cold start. Meanwhile, choosing an appropriate cold start mode is also an effective method to further enhance the cold start capability of the PEMFC [12,13]. At the present stage, the common cold start modes without auxiliary include constant current mode [14–17], constant voltage mode [18–21], and constant power mode [22–24]. In these three modes, the constant voltage mode usually operates at a low start-voltage (lower than 0.3 V) and generates more heat, which can shorten the cold start time of the

[1]Corresponding author.

Manuscript received March 12, 2021; final manuscript received September 13, 2021; published online October 13, 2021. Assoc. Editor: Steven C. DeCaluwe.

PEMFC [25,26]. Therefore, the constant voltage mode is more suitable for low-temperature applications and may be applied to fuel cell vehicles in the future [27].

Besides, the degradation levels of the PEMFC after constant voltage cold start is one of the determining factors to apply this start-up mode at low temperatures. Thus, it is important to investigate the effect of the constant voltage cold start on the durability of the PEMFC. In the present known studies, the phase transition of the water and the alternations of the temperature are the main reasons leading to the degradation of the PEMFC performance, especially the irreversible damage to the structure of the MEA [28,29]. For example, Lee et al. [30] explored the durability of the MEA in the freezing–thawing cycle. The results showed that the structure of the catalyst layer collapsed and agglomerated, and the catalyst dissolved due to repeated freezing–thawing. Oszcipok et al. [31] studied the changes in hydrophobicity of the GDL surface before and after the freezing–thawing experiment. The hydrophobicity of the cathode side decreased and the number of large hydrophobic holes increased, indicating that the void distribution of the GDL was affected by the internal water freezing. To our knowledge, the durability of the PEMFC under specific operating conditions has not been discussed in past studies. Recently, Lin et al. [32] investigated the degradation mechanism of the stack under the constant voltage cold start by the polarization curve and single cell voltage fluctuation rate. They suggested that the degradation of the PEMFC at a single cell voltage below 0.3 V was mainly caused by water freezing, which destroyed the structure of the GDL, and resulted in the shedding of Pt particles on the catalyst. However, the degradation characteristics of the PEMFC shall also be investigated at the micro-level under constant voltage mode, so as to understand the variation of the MEA in the PEMFC in-depth during the cold start process and help us to set the cold start operating parameters.

Thus, in this work, the constant voltage cold start experiment of the PEMFC has been tested repeatedly to simulate its actual operating state in the vehicle. After the cold start test, the electrochemical performance of the PEMFC has been analyzed by polarization curve, cyclic voltammetry (CV), and electrochemical impedance spectroscopy (EIS). Meanwhile, the morphological and structural changes of the MEA components have been studied utilizing the transmission electron microscope (TEM) and ion chromatography (IC). Based on the experimental results, the degradation mechanism of the PEMFC under constant voltage cold start can be obtained.

Experimental Section

Single Cell Assembly and Activation. The testing single cell was assembled with a commercial MEA (Hyplat) and the parameter of the MEA and single cell was shown in Table 1. Before the cold start experiment, an activation test of the single cell was needed to achieve its optimum performance. The stoichiometry of the air and hydrogen are both 2, the backpressure is 1.5 bar(a), the temperature of the single cell is 75 °C, and the relative humidity is 100%. The fuel cell was operated under electronic load control for 30 s at 0.8 V and 10 min at 0.3 V for a period of 4 h. After that, the polarization curve is measured.

Table 1 The parameter of the MEA and single cell

Parameter	Title
MEA	Commercial
Effective active area	25 cm^2
Pt catalyst load	Anode: 0.1 mg cm^{-2} Cathode: 0.4 mg cm^{-2}
Flow field structure	Anode: serpentine flow field Cathode: serpentine flow field
Hydrogen/air flow field	Counter flow
Channel width	1 mm
Channel height	0.8 mm
Land width	1 mm

Table 2 The test parameters of the polarization curve

	Value	
Parameter	Anode	Cathode
Stoichiometric ratio	1.2	2.5
Gas humidity	100%	100%
Gas temperature	75 °C	75 °C
Back pressure (absolute)	1 bar	1 bar

Table 3 The parameters of the galvanostatic test

	Value		
Parameter	Anode	Cathode	Single cell
Stoichiometric ratio	1.2	2.5	
Gas humidity	100%	100%	
Gas temperature	75 °C	75 °C	
Back pressure (absolute)	1 bar	1 bar	
Current			680 mA cm^{-2}

Cold Start and Galvanostatic Experimental Procedure. After activation, the anode and cathode of the PEMFC were purged by the dry nitrogen for 4 h with a flowrate of 2 L min^{-1} and 5 L min^{-1}, respectively, to ensure that the MEA would not be damaged by water freezing. Then, the PEMFC was moved into the climate chamber. Due to the low heat production of the single cell, it could only realize the cold start with the minimum temperature of −5 °C without an external auxiliary [33]. Therefore, the temperature of the climate chamber was set to −5 °C and the temperature was kept constant for 4 h. Later, the PEMFC was started at 0.1 V with a flowrate of 1.2 L min^{-1} and 2.7 L min^{-1} for the anode and cathode, respectively. After the cold start experimental procedure, the PEMFC was taken out from the climate chamber, and its electrochemical performance and characterization were tested. The polarization curve of the PEMFC was tested at 75 °C and the test parameters were exhibited in Table 2.

Finally, in order to avoid the impact of freezing on experimental results, the PEMFC was purged with nitrogen and prepared for the next cold start experiment. The cold start procedure of the PEMFC was repeated 20 times.

Besides, as a control experiment, a long-time galvanostatic test was prepared at normal operating conditions. And the parameters of the galvanostatic test are shown in Table 3.

Cold Start Experimental Test Platform. A fuel cell test platform (PEMTest50, Hephas) was used to supply the reaction gas and control the operating parameters such as backpressure, load, gas flow, and humidity of the PEMFC. And the schematic diagram of the test platform was displayed in Fig. 1. A climate chamber with a temperature range of −40 to 150 °C was adopted to adjust the temperature for the cold start experiment and simulate the subzero environment. Two 2 m cooling coils were added in the climate chamber to make sure that the temperature of the reaction gas entering into the fuel cell was consistent with the setting temperature of the climate chamber.

Characterization Analysis. The EIS of the PEMFC was measured by Autolab PGSTAT 302N electrochemical workstation (Metrohm), which used a two-electrode cell with an anode as a reference electrode. Meanwhile, the ohmic resistance and charge transfer resistance in the PEMFC could also be obtained. The

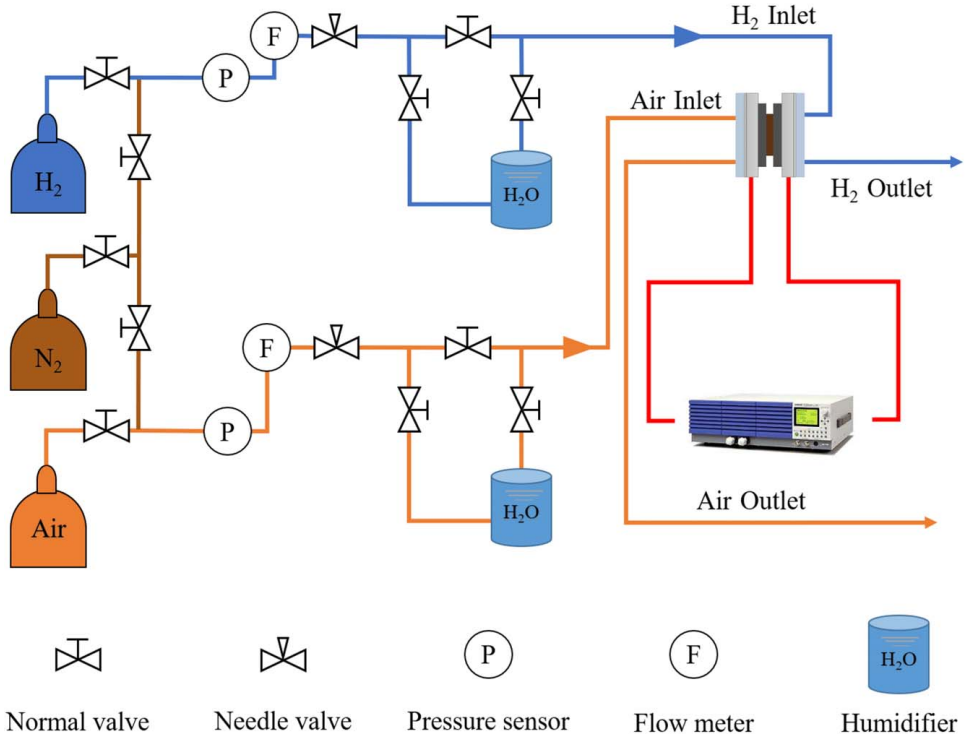

Fig. 1 The schematic diagram of the test platform

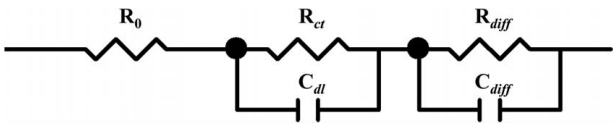

Fig. 2 The equivalent model diagram of the fuel cell

ohmic resistance reflected the ion conduction ability of the proton exchange membrane and charge transfer resistance reflected the charge transferability of the catalyst. The impedance measurements were executed in the galvanostatic mode with a frequency range of 10 kHz to 0.1 Hz, and the linear response of the system was obtained by applying an AC signal whose amplitude is 10% of the DC. Then, the impedance results were fitted by a common fuel cell EIS equivalent circuit, and the equivalent model was shown in Fig. 2.

The CV was also measured by Autolab PGSTAT 302N Electrochemical Workstation. The hydrogen and nitrogen with the relative humidity of 100% were fed into the anode and cathode, respectively, at the flowrate of 0.2 L min^{-1}. The voltage range of the CV measurement was 0.05–1.05 V and the scanning rate was 50 mV s^{-1}. After that, the H_2 crossover current was obtained according to the CV data [34] and the electrochemical surface area (ECSA) at the cathode electrode. The calculation method of ECSA is displayed in Eq. (1).

$$A_{\mathrm{ECSA}} = \frac{Q}{0.21 * M_{\mathrm{Pt}}} \tag{1}$$

A_{ECSA} is the ECSA (cm^2 mg^{-1}), Q is the total amount of electron transfer (μC), M_{pt} is the Pt load on the cathode electrode (mg), and the unit of constant is μC cm^{-2}.

The catalyst in the PEMFC before the cold start and after 20 cold starts was collected. And the morphology of the sample was obtained on a TEM (TALOS F200X, Thermo Scientific) with a voltage of 200 kV.

The PEMFC before the cold start and after 20 cold starts was tested by the test platform and the test parameters were shown in Table 4. After that, the concentration of F^- and SO_4^{2-} in the water separated from the anode and cathode of the PEMFC was analyzed using the IC method (DX-120, DIONEX).

Table 4 The test parameters of the PEMFC before and after the cold start

Parameter	Value		
	Anode	Cathode	Single cell
Stoichiometric ratio	1.2	2.5	–
Gas humidity	100%	100%	–
Gas temperature	75 °C	75 °C	–
Back pressure (absolute)	1 bar	1 bar	–
Operating voltage	–	–	0.65 V
Operating time	–	–	200 min

Results and Discussion

In this section, the influence of constant voltage cold start on the performance of PEMFC was studied by electrochemical measurement, structural characterization, and spectrum characterization, respectively.

The Constant Voltage Cold Start Characteristics and the Performance of the Proton Exchange Membrane Fuel Cell After the Cold Start. To avoid the structure damage and electrochemical performance attenuation of the MEA caused by cold start failure, a cold start experiment under the condition of −5 °C was selected [33]. The effect of the constant voltage cold start at −5 °C was shown in Fig. 3. When the PEMFC was started at 0.1 V in the constant voltage mode, the peak current density reached 1110.4 mA cm^{-2} and a large amount of heat was generated. Thus, the PEMFC could be started successfully from −5 °C. However, due to the large heat capacity of the bipolar plate, the cold start speed of the single cell was relatively slow, taking 255 s from −5 to 0 °C.

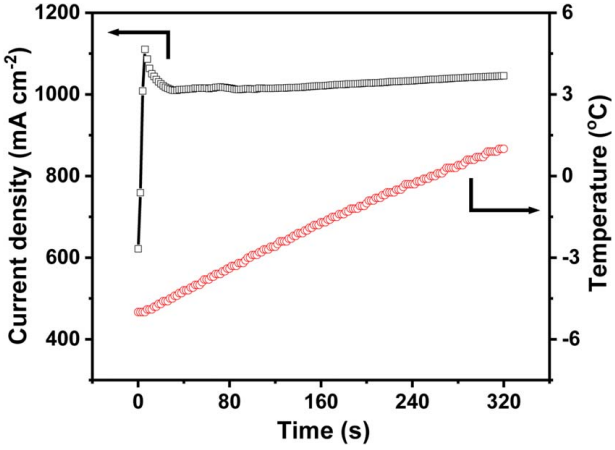

Fig. 3 Effect of the constant voltage cold start at −5 °C (starting voltage was 0.1 V)

After the cold start, the polarization and power curves of the PEMFC were tested and the performance changes of the PEMFC before and after the cold start at different times were displayed in Fig. 4. On one hand, for the power curves in Fig. 4(*a*), the power of the PEMFC decreased with the increase of the cold start times at the same current density. After 20 cold start experiments, the maximum power of the PEMFC decreased from 391.27 mW cm^{-2} before cold start to 291.20 mW cm^{-2}. Moreover, as shown in Fig. 4(*b*), when the current density was less than 300 mA cm^{-2}, the voltage of the PEMFC dropped rapidly with the increase of the cold start experiments, demonstrating that the cold start experiment would lead to the increase of electrochemical polarization of PEMFC. In other words, the catalytic activity of the catalyst in MEA was reduced.

Besides, the effects of time on the PEMFC performance at normal operating conditions were investigated and the results were exhibited in Fig. 5. During the galvanostatic test, the voltage of PEMFC did not fluctuate much which was shown in Fig. 5(*a*). Meanwhile, the polarization curve of PEMFC before and after the galvanostatic test was shown in Fig. 5(*b*), with almost no change in the curve. That is the performance of PEMFC during the galvanostatic test without significant degradation.

H_2 Crossover and Electrochemical Surface Area. Generally, H_2 crossover in PEMFC is one of the important parameters to evaluate the degradation of the membrane [35]. The larger the H_2 crossover current is, the more serious the membrane degradation is. Meanwhile, the CV measurement can be used to analyze H_2 crossover in PEMFC [34]. Thus, the CV curves of the PEMFC were tested to study the degradation of the PEMFC after the constant voltage cold start, which was exhibited in Fig. 6(*a*). Based on the

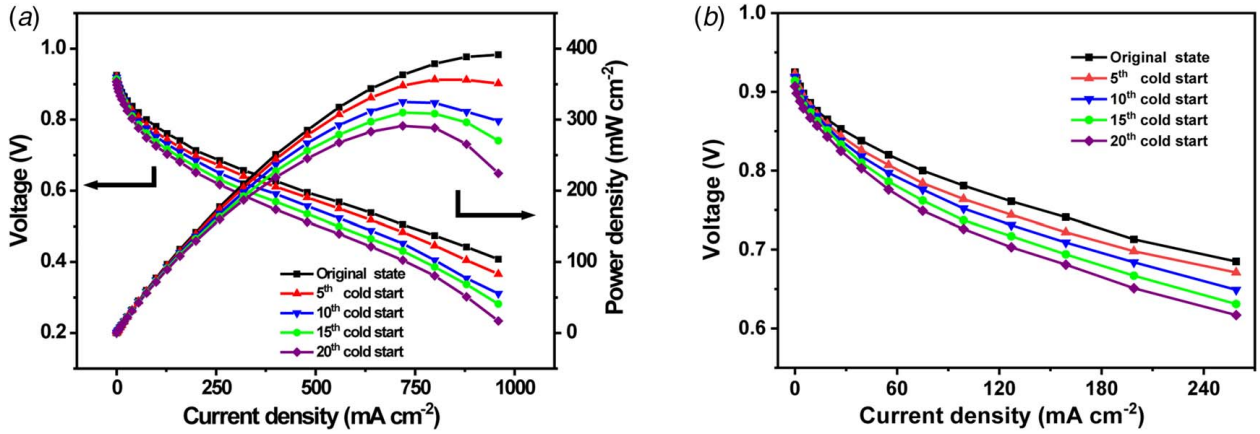

Fig. 4 (*a*) Performance changes of the PEMFC after the cold start and (*b*) polarization curve of the PEMFC after the cold start at different times (current density < 300 mA cm^{-2})

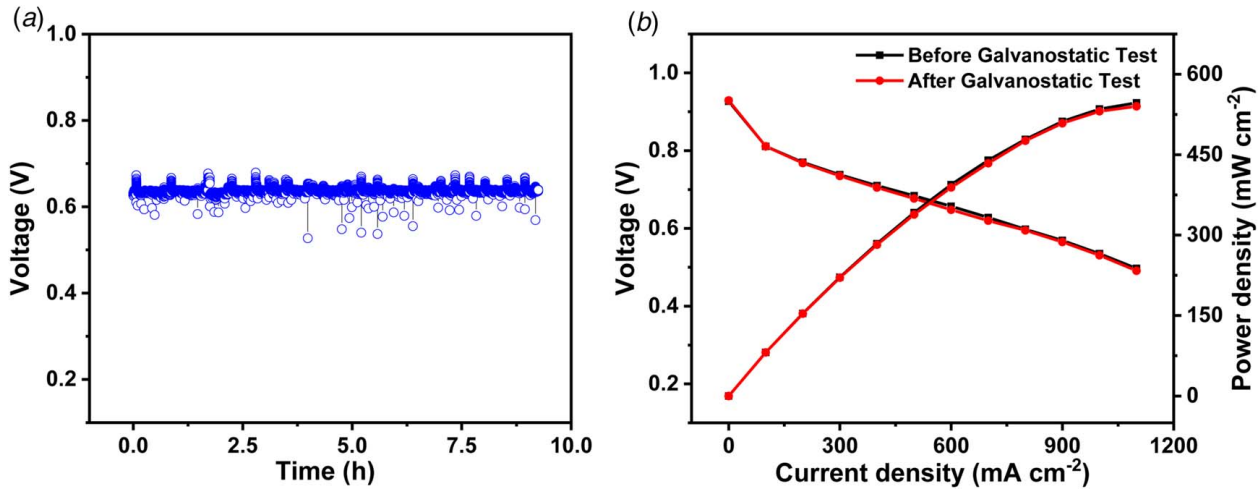

Fig. 5 (*a*) The galvanostatic test of PEMFC at 680 mA cm^{-2} and (*b*) the polarization curve of PEMFC before and after the galvanostatic test

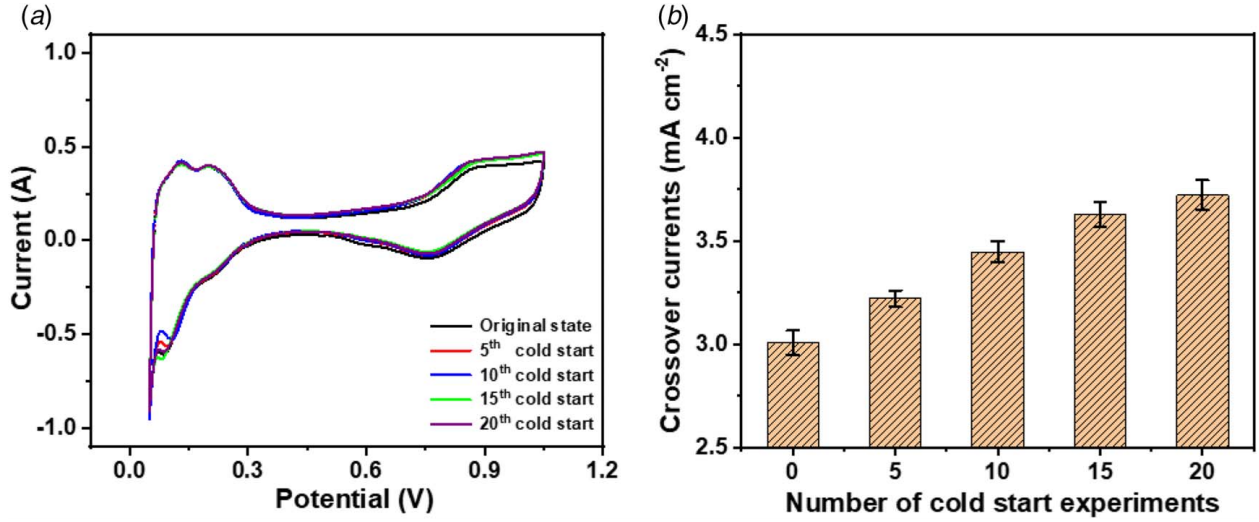

Fig. 6 (*a*) The CV curve of the PEMFC before and after the cold start at different times (voltage range is 0.05–1.05 V and the scanning rate was 50 mV s^{-1}) and (*b*) H_2 crossover current at different cold start experiment times

Table 5 The OCV of the PEMFC after different cold start experiments

Number	OCV
0	0.925 V
5	0.921 V
10	0.919 V
15	0.914 V
20	0.907 V

CV data, the H_2 crossover current was calculated according to the method in Ref. [34], and the H_2 crossover current at different cold start experiment times was demonstrated in Fig. 6(*b*). With the increase of the cold start times, the H_2 crossover current increased gradually, indicating that the amount of H_2 crossed the membrane increased. Furthermore, the H_2 crossover could be also reflected by open circuit voltage (OCV). A large H_2 leakage flux would lead to a lower OCV [36]. Table 5 shows the OCV of the PEMFC after different cold start experiments. The OCV of the PEMFC without cold start experiment was 0.925 V. However, after 20 cold start experiments, the voltage dropped to 0.907 V. Therefore, the results indicated that the H_2 crossover became more serious with the increase of the cold start times.

Besides, ECSA is one of the most important determinants that affect the performance of fuel cell catalysts. The catalysts with larger ECSA demonstrated better electrochemical performance. Thus, the ECSA of the platinum catalysts at the cathode electrode was calculated based on the CV data and the result was exhibited in Fig. 7. It could be seen clearly from Fig. 7 that the ECSA of the catalyst decreased with the increase in the number of the constant voltage cold start. Especially after 10 constant voltage cold starts, the ECSA of the PEMFC declined rapidly.

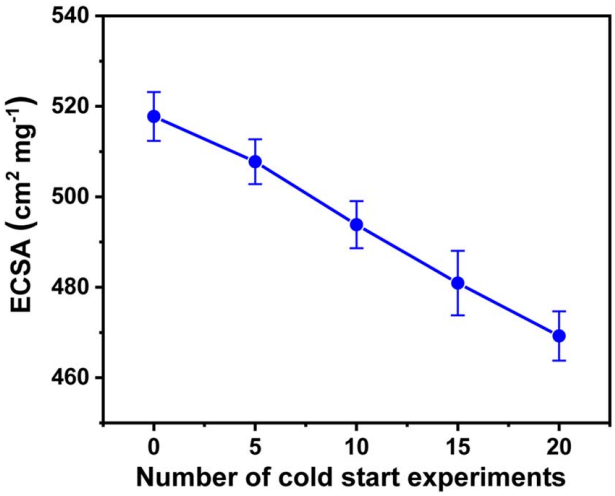

Fig. 7 The ECSA of the PEMFC before and after the cold start at different times

Electrochemical Impedance Spectra. Moreover, the degradation mechanism of the PEMFC performance could also be confirmed through EIS measurement. The ohmic resistance could reflect the proton transport capacity in the membrane. The higher the ohmic resistance is, the weaker the proton transport capacity in the membrane is. Figure 8(*a*) shows the EIS of the PEMFC after the cold start at different times. The ohmic resistance enlarged with the increase of the cold start times, which could be seen clearly in the insert diagram, illustrating a decrease in proton conductivity of the membrane caused by the constant voltage cold start.

Additionally, the charge transfer resistance could reflect the rate of charge transfer on the electrode surface. A greater charge transfer resistance means a slower charge transfer rate at the electrode surface. Thus, the charge transfer resistances of the PEMFC after the cold start at different times were fixed. As shown in Fig. 8(*b*), the increased charge transfer resistance indicated that the electrochemical reaction activity of the platinum catalyst has deteriorated.

Transmission Electron Microscope. The TEM images of the catalyst in the MEA before and after constant voltage cold start were displayed in Fig. 9. It could be seen clearly that the particle size of the platinum catalyst on the anode and cathode was about 4 nm without constant voltage cold start in Figs. 9(*a*) and 9(*b*). However, after 20 cold start experiments, the platinum catalysts on both anode and cathode were agglomerated, which was exhibited in Figs. 9(*c*) and 9(*d*). Especially on the cathode side shown in Fig. 9(*d*), the agglomeration degree of the platinum catalysts was much more serious than that on the anode side, and the particle size of the platinum catalyst enlarged. Based on the electrochemical characterization results mentioned above, the degradation of the platinum catalyst performance should be demonstrated that high operating current caused the agglomeration of catalyst particles which led to the decrease of the electrochemical active area [37].

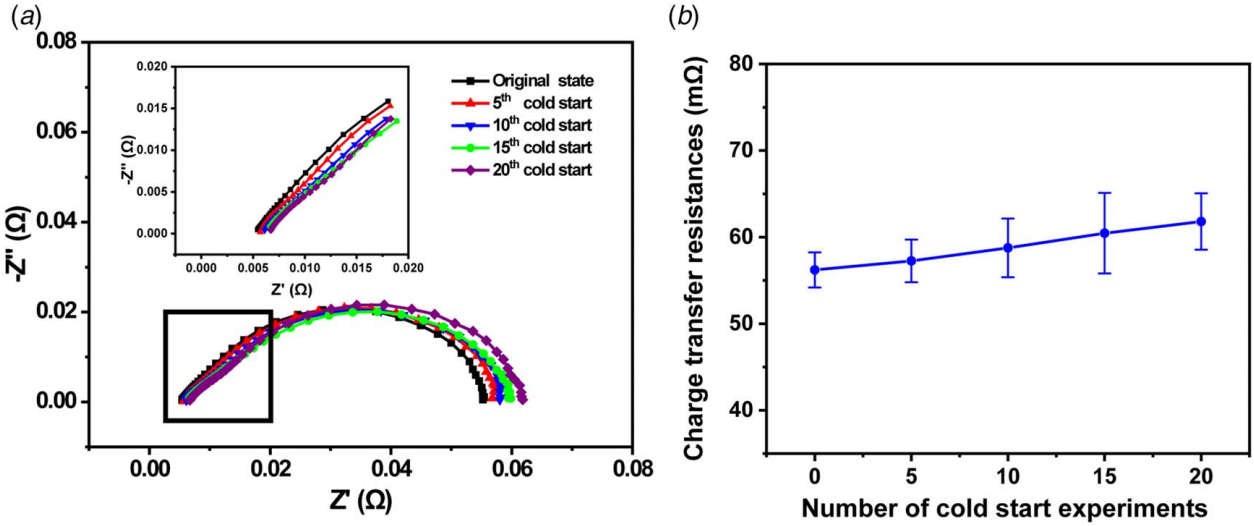

Fig. 8 (*a*) The EIS of the PEMFC after the cold start at different times and (*b*) the charge transfer resistances of the PEMFC after the cold start at different times

Ion Chromatography. To further verify the degradation of the membrane, the PEMFC before the cold start and after 20 cold starts was tested by the test platform. After testing for 200 min, the water separated from the cathode and anode was collected, and the composition of the ions in water was analyzed by the IC method. Among them, the water separated from the cathode mainly came from the electrochemical reaction, and the water separated from the anode mainly came from the cathode. The concentration of F^- and SO_4^{2-} ions in water represents the degree of membrane decomposition. A high ion concentration indicated serious damage to the

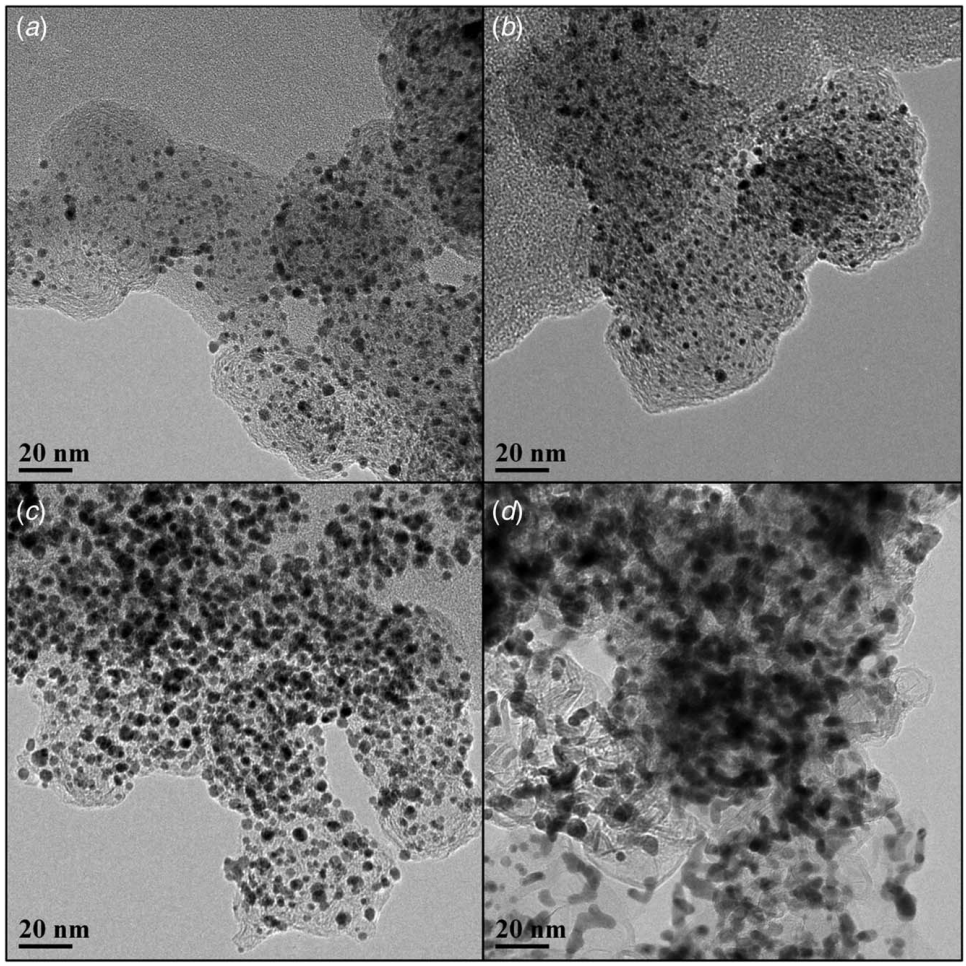

Fig. 9 TEM images of the anode and cathode catalysts in the MEA before and after the cold start. (*a*) The catalyst in anode before the cold start, (*b*) the catalyst in cathode before the cold start, (*c*) the catalyst in anode after 20 cold starts, and (*d*) the catalyst in cathode after 20 cold starts.

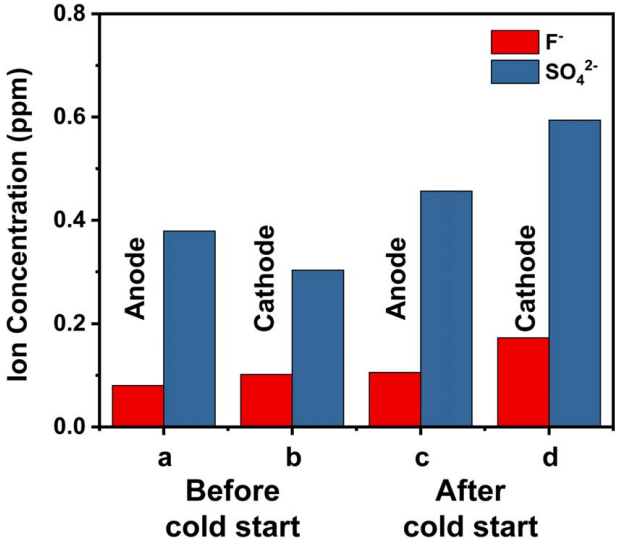

Fig. 10 IC results of ionic components in water separated from the anode and cathode of the PEMFC after testing for 200 min at 0.65 V. (*a*) The water separated from the anode of the PEMFC before the cold start, (*b*) the water separated from the cathode of the PEMFC before the cold start, (*c*) the water separated from the anode after 20 cold starts, and (*d*) the water separated from the cathode after 20 cold starts.

membrane. The concentration of F^- and SO_4^{2-} ions in the water separated from the anode and cathode of the PEMFC was displayed in Fig. 10. The F^- and SO_4^{2-} ion concentration in the water collected from the cold-started fuel cell, which was displayed in Figs. 10(*c*) and 10(*d*), was obviously higher than that from the non-cold-started fuel cell, illustrating in Figs. 10(*a*) and 10(*b*), under the same operating conditions and running time. Especially at the cathode side shown in Figs. 10(*b*) and 10(*d*), the concentrations of F^- and SO_4^{2-} increased more significantly after the cold start. Combined with H_2 crossover current results in Fig. 6(*b*) and the EIS results in Fig. 8(*a*), it could be proved that high operating current led to the non-uniform current distribution of single fuel cell along the gas channel more severe, causing local overheating of the membrane, which led to the membrane destruction and H_2 crossover [35]. Meanwhile, the crossover H_2 accelerates the degradation of the membrane, and the proton transmission channel was damaged, resulting in the reduction of proton conductivity.

Conclusions

In this work, the characteristic of the PEMFC in the constant voltage cold start at 0.1 V is studied. After the repeatedly cold start, the output performance of the PEMFC decreased significantly. Then the characterization measurement of the PEMFC is investigated after the constant voltage cold start test. EIS and CV measurements evidence that frequent constant voltage cold start can cause irreversible damage to the platinum catalyst and membrane of the PEMFC. And TEM and IC measurements further confirm that the constant voltage cold start of the PEMFC can cause platinum catalyst agglomeration and membrane polymer structure decomposition. In conclusion, the degradation mechanism of the PEMFC at the constant voltage cold start is declared that high operating current leads to the non-uniform current distribution of single fuel cell along the gas channel more severe, causing local overheating of the membrane, which promotes the crossover of H_2 and results in the decomposition of membrane polymer structure. Moreover, the high current also causes the degradation of the catalyst layer. Above all, this study proves that the durability of PEMFC can be shortened by the constant voltage cold start at 0.1 V, which provides a reference for the development of the PEMFC cold start control strategy.

Acknowledgment

This work has been funded by the National Natural Science Foundation of China (No. 52077157).

Conflict of Interest

There are no conflicts of interest.

Data Availability Statement

The authors attest that all data for this study are included in the paper.

References

[1] Gurz, M., Baltacioglu, E., Hames, Y., and Kaya, K., 2017, "The Meeting of Hydrogen and Automotive: A Review," Int. J. Hydrogen Energy, **42**(36), pp. 23334–23346.
[2] Amamou, A., Kandidayeni, M., Macias, A., Boulon, L., and Kelouwani, S., 2020, "Efficient Model Selection for Real-Time Adaptive Cold Start Strategy of a Fuel Cell System on Vehicular Applications," Int. J. Hydrogen Energy, **45**(38), pp. 19664–19675.
[3] Li, L., Wang, S., Yue, L., and Wang, G., 2019, "Cold-Start Icing Characteristics of Proton-Exchange Membrane Fuel Cells," Int. J. Hydrogen Energy, **44**(23), pp. 12033–12042.
[4] Zhou, Y., Luo, Y., Yu, S., and Jiao, K., 2014, "Modeling of Cold Start Processes and Performance Optimization for Proton Exchange Membrane Fuel Cell Stacks," J. Power Sources, **247**, pp. 738–748.
[5] Mao, L., and Wang, C.-Y., 2007, "Analysis of Cold Start in Polymer Electrolyte Fuel Cells," J. Electrochem. Soc., **154**(2), pp. B139–B146.
[6] Hirakata, S., Mochizuki, T., Uchida, M., Uchida, H., and Watanabe, M., 2013, "Investigation of the Effect of Pore Diameter of Gas Diffusion Layers on Cold Start Behavior and Cell Performance of Polymer Electrolyte Membrane Fuel Cells," Electrochim. Acta, **108**, pp. 304–312.
[7] Mishler, J., Wang, Y., Mukherjee, P. P., Mukundan, R., and Borup, R. L., 2012, "Subfreezing Operation of Polymer Electrolyte Fuel Cells: Ice Formation and Cell Performance Loss," Electrochim. Acta, **65**, pp. 127–133.
[8] Tajiri, K., Tabuchi, Y., Kagami, F., Takahashi, S., Yoshizawa, K., and Wang, C.-Y., 2007, "Effects of Operating and Design Parameters on PEFC Cold Start," J. Power Sources, **165**(1), pp. 279–286.
[9] Jiao, K., Alaefour, I. E., Karimi, G., and Li, X., 2011, "Cold Start Characteristics of Proton Exchange Membrane Fuel Cells," Int. J. Hydrogen Energy, **36**(18), pp. 11832–11845.
[10] Tabe, Y., Saito, M., Fukui, K., and Chikahisa, T., 2012, "Cold Start Characteristics and Freezing Mechanism Dependence on Start-Up Temperature in a Polymer Electrolyte Membrane Fuel Cell," J. Power Sources, **208**, pp. 366–373.
[11] Lin, R., Lin, X., Weng, Y., and Ren, Y., 2015, "Evolution of Thermal Drifting During and After Cold Start of Proton Exchange Membrane Fuel Cell by Segmented Cell Technology," Int. J. Hydrogen Energy, **40**(23), pp. 7370–7381.
[12] Yan, Q., Toghiani, H., Lee, Y.-W., Liang, K., and Causey, H., 2006, "Effect of Sub-Freezing Temperatures on a PEM Fuel Cell Performance, Startup and Fuel Cell Components," J. Power Sources, **160**(2), pp. 1242–1250.
[13] Oberholzer, P., Boillat, P., Siegrist, R., Perego, R., Kästner, A., Lehmann, E., Scherer, G. G., and Wokaun, A., 2011, "Cold-Start of a PEFC Visualized With High Resolution Dynamic In-Plane Neutron Imaging," J. Electrochem. Soc., **159**(2), pp. B235–B245.
[14] Ko, J., and Ju, H., 2013, "Effects of Cathode Catalyst Layer Design Parameters on Cold Start Behavior of Polymer Electrolyte Fuel Cells (PEFCs)," Int. J. Hydrogen Energy, **38**(1), pp. 682–691.
[15] Jung, H.-M., and Um, S., 2011, "An Experimental Feasibility Study of Vanadium Oxide Films on Metallic Bipolar Plates for the Cold Start Enhancement of Fuel Cell Vehicles," Int. J. Hydrogen Energy, **36**(24), pp. 15826–15837.
[16] Luo, Y., Guo, Q., Du, Q., Yin, Y., and Jiao, K., 2013, "Analysis of Cold Start Processes in Proton Exchange Membrane Fuel Cell Stacks," J. Power Sources, **224**, pp. 99–114.
[17] Miao, Z., Yu, H., Song, W., Hao, L., Shao, Z., Shen, Q., Hou, J., and Yi, B., 2010, "Characteristics of Proton Exchange Membrane Fuel Cells Cold Start With Silica in Cathode Catalyst Layers," Int. J. Hydrogen Energy, **35**(11), pp. 5552–5557.
[18] Meng, H., 2008, "A PEM Fuel Cell Model for Cold-Start Simulations," J. Power Sources, **178**(1), pp. 141–150.
[19] Lim, S.-J., Park, G.-G., Park, J.-S., Sohn, Y.-J., Yim, S.-D., Yang, T.-H., Hong, B. K., and Kim, C.-S., 2010, "Investigation of Freeze/Thaw Durability in Polymer Electrolyte Fuel Cells," Int. J. Hydrogen Energy, **35**(23), pp. 13111–13117.

[20] Jiao, K., Alaefour, I. E., Karimi, G., and Li, X., 2011, "Simultaneous Measurement of Current and Temperature Distributions in a Proton Exchange Membrane Fuel Cell During Cold Start Processes," Electrochim. Acta, **56**(8), pp. 2967–2982.
[21] Lin, R., Weng, Y., Lin, X., and Xiong, F., 2014, "Rapid Cold Start of Proton Exchange Membrane Fuel Cells by the Printed Circuit Board Technology," Int. J. Hydrogen Energy, **39**(32), pp. 18369–18378.
[22] Blackwelder, M. J., and Dougal, R. A., 2004, "Power Coordination in a Fuel Cell-Battery Hybrid Power Source Using Commercial Power Controller Circuits," J. Power Sources, **134**(1), pp. 139–147.
[23] Thounthong, P., Raël, S., and Davat, B., 2006, "Control Strategy of Fuel Cell/Supercapacitors Hybrid Power Sources for Electric Vehicle," J. Power Sources, **158**(1), pp. 806–814.
[24] Oszcipok, M., Zedda, M., Hesselmann, J., Huppmann, M., Wodrich, M., Junghardt, M., and Hebling, C., 2006, "Portable Proton Exchange Membrane Fuel-Cell Systems for Outdoor Applications," J. Power Sources, **157**(2), pp. 666–673.
[25] Schießwohl, E., von Unwerth, T., Seyfried, F., and Brüggemann, D., 2009, "Experimental Investigation of Parameters Influencing the Freeze Start Ability of a Fuel Cell System," J. Power Sources, **193**(1), pp. 107–115.
[26] Jiao, K., and Li, X., 2010, "Cold Start Analysis of Polymer Electrolyte Membrane Fuel Cells," Int. J. Hydrogen Energy, **35**(10), pp. 5077–5094.
[27] Henao, N., Kelouwani, S., Agbossou, K., and Dubé, Y., 2012, "Proton Exchange Membrane Fuel Cells Cold Startup Global Strategy for Fuel Cell Plug-In Hybrid Electric Vehicle," J. Power Sources, **220**, pp. 31–41.
[28] Hwang, G. S., Kim, H., Lujan, R., Mukundan, R., Spernjak, D., Borup, R. L., Kaviany, M., Kim, M. H., and Weber, A. Z., 2013, "Phase-Change-Related Degradation of Catalyst Layers in Proton-Exchange-Membrane Fuel Cells," Electrochim. Acta, **95**, pp. 29–37.
[29] Alink, R., Gerteisen, D., and Oszcipok, M., 2008, "Degradation Effects in Polymer Electrolyte Membrane Fuel Cell Stacks by Sub-Zero Operation—An In Situ and Ex Situ Analysis," J. Power Sources, **182**(1), pp. 175–187.
[30] Lee, S.-Y., Kim, H.-J., Cho, E., Lee, K.-S., Lim, T.-H., Hwang, I. C., and Jang, J. H., 2010, "Performance Degradation and Microstructure Changes in Freeze–Thaw Cycling for PEMFC MEAs With Various Initial Microstructures," Int. J. Hydrogen Energy, **35**(23), pp. 12888–12896.
[31] Oszcipok, M., Riemann, D., Kronenwett, U., Kreideweis, M., and Zedda, M., 2005, "Statistic Analysis of Operational Influences on the Cold Start Behaviour of PEM Fuel Cells," J. Power Sources, **145**(2), pp. 407–415.
[32] Lin, R., Zhu, Y., Ni, M., Jiang, Z., Lou, D., Han, L., and Zhong, D., 2019, "Consistency Analysis of Polymer Electrolyte Membrane Fuel Cell Stack During Cold Start," Appl. Energy, **241**, pp. 420–432.
[33] Hishinuma, Y., Chikahisa, T., Kagami, F., and Ogawa, T., 2004, "The Design and Performance of a PEFC at a Temperature Below Freezing," JSME Int. J. Ser. B, **47**(2), pp. 235–241.
[34] Génevé, T., Turpin, C., Régnier, J., Rallières, O., Verdu, O., Rakotondrainibe, A., and Lombard, K., 2017, "Voltammetric Methods for Hydrogen Crossover Diagnosis in a PEMFC Stack," Fuel Cells, **17**(2), pp. 210–216.
[35] Francia, C., Ijeri, V. S., Specchia, S., and Spinelli, P., 2011, "Estimation of Hydrogen Crossover Through Nafion® Membranes in PEMFCs," J. Power Sources, **196**(4), pp. 1833–1839.
[36] Arato, E., and Costa, P., 2006, "Transport Mechanisms and Voltage Losses in PEMFC Membranes and at Electrodes: A Discussion of Open-Circuit Irreversibility," J. Power Sources, **159**(2), pp. 861–868.
[37] Wilson, M. S., Garzon, F. H., Sickafus, K. E., and Gottesfeld, S., 1993, "Surface Area Loss of Supported Platinum in Polymer Electrolyte Fuel Cells," J. Electrochem. Soc., **140**(10), pp. 2872–2877.